

# A Climatic Index for Aeolian Desertification in Northern China and its Application to Dust Storm Frequency

Zhen-Ting Wang<sup>1,2\*</sup>, Ying-Ying Wu<sup>1,3</sup>, Yu Ren<sup>4</sup>

<sup>1</sup>Key Laboratory of Desert and Desertification, Northwest Institute of Eco-Environment and Resources, CAS, China; <sup>2</sup>Research Station of Gobi Desert Ecology and Environment of Gansu Province, China; <sup>3</sup>University of Chinese Academy of Sciences, Beijing, China; <sup>4</sup>College of Geography and Environmental Science, Northwest Normal University, China

## ABSTRACT

Aeolian desertification is the dominant desertification type in northern China. The robust relations between climate variables and desertification indicators must be established while predicting the future desertification trends by using climate models. Vegetations are sensitive to climate change and desertification simultaneously. A basic feature of aeolian desertification process in northern China is that aeolian sand and dust activities proceed the vegetation growth season in the same year. In this study, such a lagging effect of desertification to climate change is described by the wind erosion and vegetation growth models. A non-dimensional aeolian desertification index composed of wind speed, precipitation and temperature is constructed. Its applicability is confirmed by the temporal trends of dust storm frequency in the dust source regions.

**Keywords:** Aeolian desertification; Climate variables; Dust storm frequency; Northern China

## INTRODUCTION

Desertification is land degradation at arid, semiarid and dry sub-humid areas resulting from various factors, including climatic variations and human activities UNCCD (1994). The effects of future climate change on desertification are of general interest [1,2]. A number of robust models can predict climate variables such as precipitation and temperature under different future emission scenarios [3,4]. Desertification can be represented by many indicators including ground surface albedo, soil organic matter and grain size distribution, vegetation cover, dust emission flux and dust storm frequency etc. [5]. However, the relations between climate variables and desertification indicators have not been well established, although the ratio of precipitation to potential evapotranspiration was used to define meteorological drought and assess desertification [6-8].

Desertification is a serious threat to China where aeolian desertification, water erosion, salinization, and freeze-thaw desertification take place frequently. Aeolian desertification is the dominant desertification type in northern China [9,10]. Since the formation and evolution of dune fields are closely related to climatic variables, desertification trends were previously estimated by the dune mobility index [11], in which the annual duration of aeolian

sand transport was taken into account. Obviously, desertification does not always occur in dunefields. The entrainment, transport and deposition of sand and dust by wind are often associated with the desertification of farmlands and steppes. Specially dust storm directly reflects the dynamical process of severe desertification. A statistical analysis of the data recorded by 129 meteorological stations in northern China during 1960-2007 showed that the predominant variables affecting dust storm frequency are wind speed, temperature and precipitation [12,13]. However, the detailed mechanisms behind the correlation relations between climatic variables and dust storm frequency remain unclear. In this study, a non-dimensional climatic index for aeolian desertification is found using these three variables, and its application to dust storm frequency is displayed.

## MATERIALS AND METHODS

### Index for aeolian desertification

The modes of particle motion in aeolian activities are traditionally classified as suspension, saltation and creep. Most of the mass and energy are transported by saltation. A widely used saltation formula is Lettau and Lettau (1978) [14],

**Correspondence to:** Zhen-Ting Wang, Key Laboratory of Desert and Desertification, Northwest Institute of Eco-Environment and Resources, CAS, China, E-mail: wangzht@lzu.edu.cn.

**Received:** Septemehr 30, 2021; **Accepted:** October 15, 2021; **Published:** October 25, 2021

**Citation:** Wang ZT, Wu YY, Ren Y (2021) A Climatic Index for Aeolian Desertification in Northern China and its Application to Dust Storm Frequency. J Climatol Weath Forecast. 9:306.

**Copyright:** © 2021 Wang ZT, et al. This is an open-access article distributed under the terms of the Creative Commons Attribution License, which permits unrestricted use, distribution, and reproduction in any medium, provided the original author and source are credited.

$$q = \begin{cases} 0 & \text{if } u_* \leq u_{*t} \\ c_0 \frac{\rho}{g} \sqrt{\frac{d}{D}} u_*^3 \left(1 - \frac{u_{*t}}{u_*}\right) & \text{if } u_* > u_{*t} \end{cases} \quad (1)$$

where  $q$  is saltation flux,  $c_0$  and  $D$  are two constants,  $\rho$ ,  $g$ ,  $d$ ,  $u_*$ ,  $u_{*t}$  are air density, gravity acceleration, sand grain size, friction speed, and threshold friction speed, respectively. The timescales of saltation events are hourly or daily. Whereas climate changes in the timescale of month or year at least. Given a bare, loose and dry land, the annual saltation flux per unit width can be written as,

$$Q_0 = \int_0^{T_0} q dt \quad (2)$$

Where  $T_0$  is equal to one year, the subscript of "0" denotes the current year.

From Equation (1), Equation (2), the wind speed effect of the  $i$ -th year is extracted,

$$Q_0 \propto U_i = \int_0^{T_i} U^3 \left(1 - \frac{U_t}{U}\right) dt \quad (3)$$

Where  $U$  ( $>U_t$ ) is the 10-meter wind speed measured by the meteorological station,  $U_t$  is the corresponding threshold wind speed.  $U_i$  is analogous to drift potential [15] Equation (3). It decreases with the averaging time of wind speed [16,17] because saltation is highly intermittent [10,18]. In the following calculation, the averaging time of wind speed and the threshold wind speed is set as 24 h and 4.5 m/s, respectively.

For a vegetated land, the annual saltation flux is,

$$Q_0 = Q_0 \left(1 - \frac{C}{C_s}\right) \quad (4)$$

Where  $C$  is vegetation coverage,  $C_s$  is a threshold above which there is no saltation [19] Equation (4).

We assume that vegetation coverage  $C$  is proportional to the above-ground biomass  $M_0$ ,

$$c \propto M_0 = M_0^a + M_0^p \quad (5)$$

Where  $M_0^a$  and  $M_0^p$  are the above-ground biomasses of annuals and perennials Equation (5). There is a lag time between aeolian desertification and vegetation growth in northern China. Aeolian sand and dust activities often occur from March to May. The growing season of vegetation in summer. The dead annuals of last year and non-green perennials protect the current land surface against wind erosion. This fact can be expressed as,

$$M_0^a \propto R_{-1}^a T_{-1} \quad (6a)$$

$$M_0^p = \alpha M_{-1}^p + \alpha R_{-1}^p T_{-1} = \alpha^n M_{-n}^p + \sum_{i=1}^n \alpha^i R_{-i}^p T_{-i} \quad (6b)$$

where  $\alpha$  is a positive constant less than 1,  $R_p^a$  and  $R_p^p$  are the annual growth rates of annuals and perennials in the  $i$ -th year. There are many functional forms for modeling plant growth [20]. For simplicity, the linear growth model is selected in Equation (6).

From Equation (5) and (6), we have,

$$M_0 \approx \alpha R_{-1}^a T_{-1} + \sum_{i=1}^n \alpha^i R_{-i}^p T_{-i} \quad (7)$$

According to the expression of net primary production rate [21], the annual growth rates can be described by several climatic variables Equation (7),

$$R_i^a = C_a \sum_{j=1}^{12} \frac{p_j^a}{p_0} \exp \left[ - \left( \frac{\bar{T}_j - T_{opt}}{T_{opt}} \right)^2 \right] \quad (8a)$$

$$R_i^p = C_p \sum_{j=1}^{12} \frac{p_j^p}{p_0} \exp \left[ - \left( \frac{\bar{T}_j - T_{opt}}{T_{opt}} \right)^2 \right] \quad (8b)$$

where  $C_a$  and  $C_p$  are two constants,  $p_j^a$  and  $p_j^p$  are the daily summed precipitations for the growths of annuals and perennials in the  $j$ -th month,  $p_0$  is a characteristic precipitation for non-dimensionalizing,  $\bar{T}_j$  is the monthly mean temperature,  $T_{opt}$  is the optimal temperature for plant growth. The expressions of  $R_i^a$  and  $R_i^p$  in Equation (8) are simplified from the regional vegetation model developed by [21]. For the desert steppes in north-west China, perennial shrubs are dominant plants responsible for surface stabilization. The sap flow measurements revealed that rainfall events larger than a threshold  $p_c$  can effectively influence the growth of desert shrubs [22]. Hence the precipitations of  $p_j^p$  and  $p_j^a$  can be computed as follows,

$$p_i^p = \begin{cases} 0 & \text{if } p \leq p_c \\ p - p_c & \text{if } p > p_c \end{cases} \quad (9a)$$

$$p_i^a = \begin{cases} p & \text{if } p \leq p_c \\ p_c & \text{if } p > p_c \end{cases} \quad (9b)$$

where  $p_c = 5$  mm,  $p$  is the rainfall of one event. For the typical steppes in north-east China, the dominant plants are perennial herbs. So it is assumed that  $p_j^p = p$  and  $p_j^a = 0$  there. The other parameters in Equation (9) are  $C_a = C_p = 1$ ,  $p_0 = 50$  mm,  $T_{opt} = 20^\circ\text{C}$ . The effects of temperature and precipitation in that month are neglected if  $\bar{T}_j < 5^\circ\text{C}$ .

$$\bar{U}_i = \frac{U_i - U_i | \min}{U_i | \max - U_i | \min} \quad (10a)$$

$$\bar{M}_0 = \frac{M_0 - M_0 | \min}{M_0 | \max - M_0 | \min} \quad (10b)$$

$U_i$  and  $M_0$  are normalized by their extremes, where "max" and "min" represent the maximum and minimum values.

$\bar{M}_0$  quantifies the effects of precipitation and temperature Equation (10). Based upon Equation (3) Equation (5), a climatic index for aeolian desertification can be constructed,

$$I = \bar{U}_i (1 - \bar{M}_0) \quad (11)$$

## RESULTS

### Application to dust storm frequency

The dataset of dust storm time series in northern China was established about ten years ago, based on a combining criterion of visibility, wind speed, and the weather process [23,24]. It offers high-quality data for many subsequent studies [25-27]. The dust storm dataset in 1954-2007 and the daily surface climate data were all downloaded from the China Meteorological Data Sharing Service System. Here the climatic index of Equation (11) is applied to analyze 17 dust storm frequency (number/year) measured in the dust sources regions; see (Figure 1) for the locations of meteorological stations. These stations are roughly uniformly

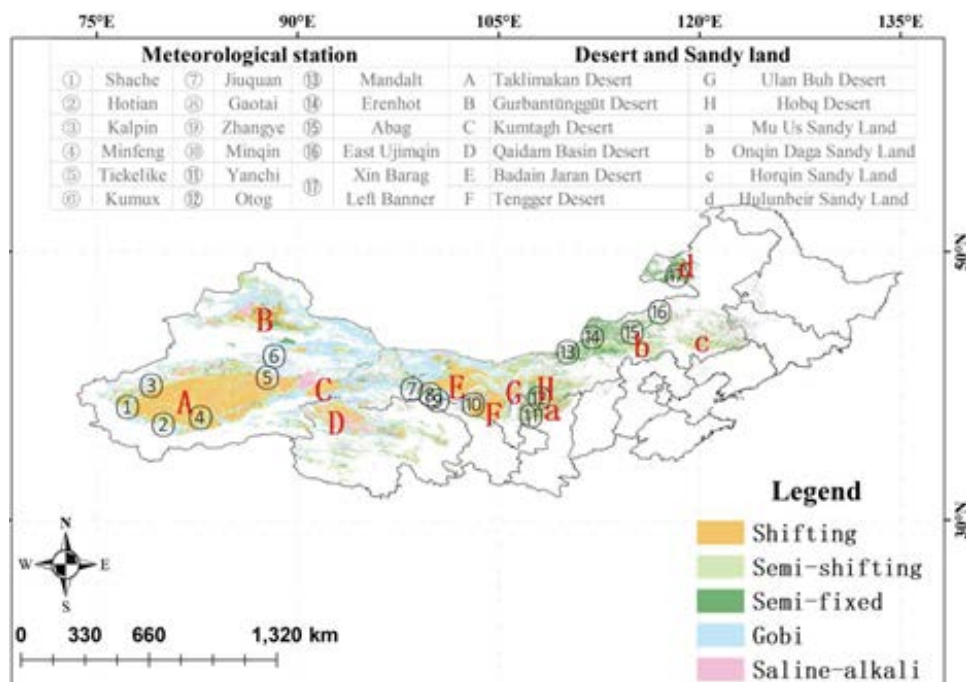


Figure 1: Locations of the meteorological stations in the map of desert and sandy land of China.

distributed in the arid and semi-arid areas of northern China.

The time series can be decomposed into the trend and fluctuation components,

$$I = I_0 + I' \tag{12a}$$

$$N = N_0 + N' \tag{12b}$$

where N is dust storm frequency,  $I_0$  and  $N_0$  are trends,  $I'$  and  $N'$  are fluctuations. Such decompositions are easily performed by the complete ensemble empirical mode decomposition adaptive noise code available at <http://perso.ens-lyon.fr/patrick.flandrin/emd.html>.  $N_0$  should synchronously change with  $I_0$  if the climatic index I is applicable. A simple relation is linear,

$$N_0 = aI_0 + b \tag{13}$$

where a and b are two fitting parameters. The subset of dust storm frequency during 1980-2005 is investigated because the measurement standard of dust visibility was revised in 1980 (Table 1).

Table 1: Parameters in the linear fitting between the trends of dust storm frequency and climatic index.

Meteorological Station	Location	$\alpha$	n	a	b	$R^2$
1 Shache	(77°16'E,38°26'N)	0.9	18	0.82	0.153	0.841
2 Hotian	(79°56'E,37°8'N)	0.98	16	1.89	0.06	0.798
3 Kalpin	(79°3'E,40°30'N)	0.77	7	1.31	0.127	0.977
4 Minfeng	(82°43'E,37°4'N)	0.97	16	1.02	0.103	0.87
5 Tiekelike	(87°42'E,40°38'N)	0.93	2	0.63	0.3	0.883
6 Kumux	(88°13'E,42°14'N)	0.97	16	0.84	0.084	0.978
7 Jiuquan	(98°29'E,39°46'N)	0.97	2	1.77	-0.106	0.772
8 Gaotai	(99°50'E,39°22'N)	0.48	1	1.02	0.016	0.95
9 Zhangye	(100°26'E,38°56'N)	0.95	2	1.16	0.013	0.697
10 Minqin	(103°5'E,38°38'N)	0.98	3	1.83	-0.148	0.983

11 Yanchi	(107°24'E,37°47'N)	0.94	5	1.48	-0.055	0.922
12 Otog	(107°59'E,39°6'N)	0.98	1	0.48	0.202	0.991
13 Mandalt	(110°8'E,42°32'N)	0.85	14	4.57	-0.883	0.936
14 Erenhot	(111°58'E,43°39'N)	0.93	10	0.38	0.278	0.449
15 Abag	(114°57'E,44°1'N)	0.85	4	0.34	0.316	0.258
16 East Ujimqin	(116°58'E,45°31'N)	0.81	2	0.55	0.114	0.722
Xin Barag						
17 Left Banner	(118°16'E,48°13'N)	0.97	8	0.88	0.02	0.977

1 lists all fitting parameters including  $\alpha$  and n in Equation (7) and a and b in Equation (13).  $R_2$  is the goodness of fit. The positive values of support the hypothesis that  $N_0$  and  $I_0$  vary synchronously. The lags of aeolian desertification to climate change range from 1 to 18 years. Three modern dust source regions are the Taklimakan Desert, the Hexi Corridor and western Inner Mongolia Plateau, and the central Inner Mongolia Plateau [25]. The meteorological stations of Nos. 1-6, 7-10, and 11-17 in Figure 1 are set up in these three regions, respectively. The landscapes of Nos. 13-17 are typical steppes. The changes of dust storm 145 frequency N, climatic index I and their trends  $N_0$  and  $I_0$  with time of three sites, Minfeng, Zhangye, and Erenhot namely, are plotted in Figure 2. Although the detailed temporal curve shapes of N and I do not identical, their trends of  $N_0$  and  $I_0$  are similar to each other. This demonstrates that the climatic index of Equation (11) is reasonable and thus suitable for prescribing the desertification in northern China. It should be pointed out that the climatic index is derived from the fundamental principles of aeolian and vegetation dynamics. In the current study, only the crucial factors are focused on. In addition to wind speed, precipitation and temperature, other variables such as radiation, evapotranspiration and soil water have influences on desertification. The more advanced climatic indexes should embody them in the future.

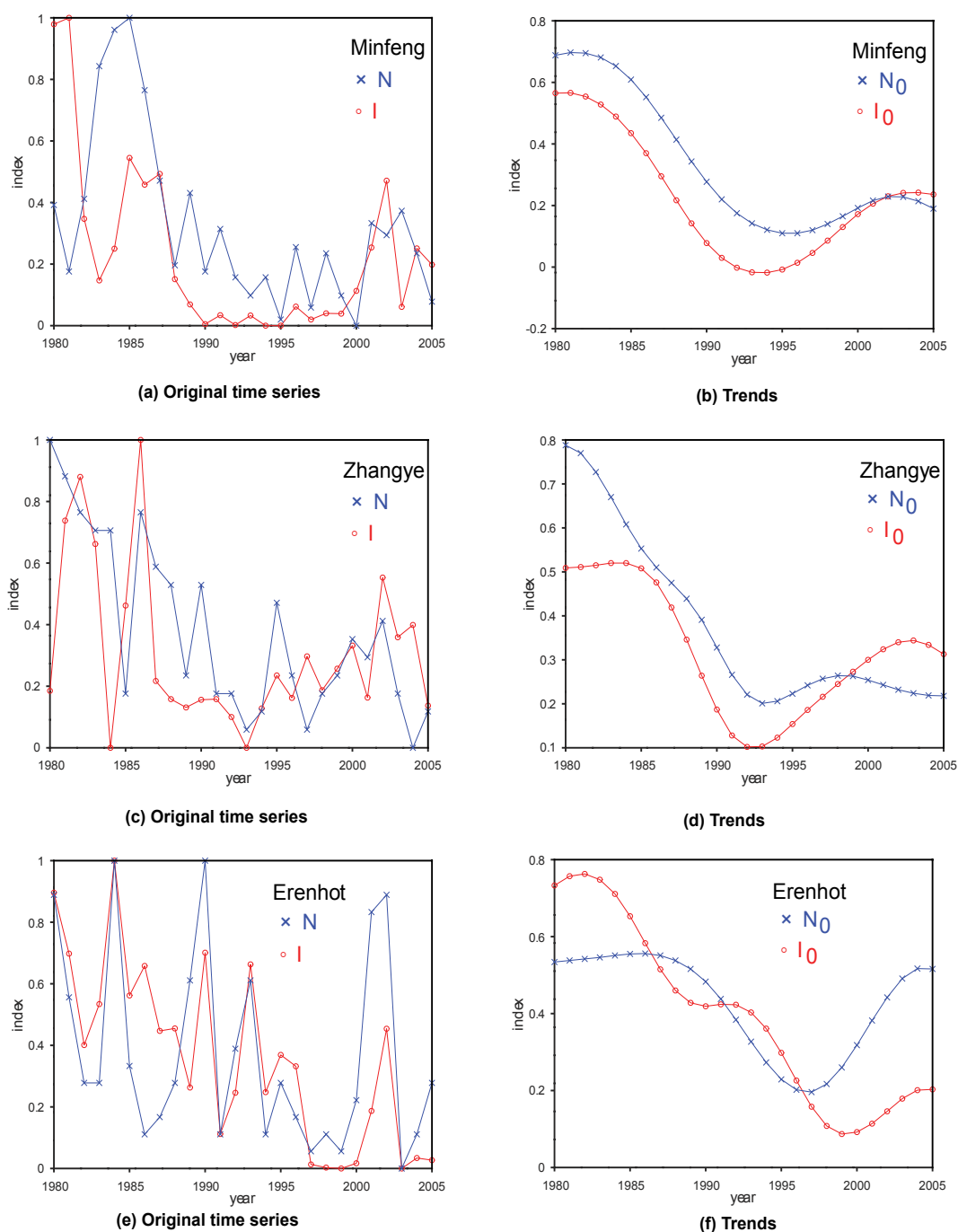


Figure 2: Changes of dust storm frequency  $N$ , climatic index  $I$  and their trends  $N_0$  and  $I_0$  with time.

## CONCLUSION

Aeolian desertification is the dominant desertification type in northern China. A basic fact is that aeolian sand and dust activities proceed the vegetation growing season in the same year. Consequently, the surface is generally protected to resist wind erosion by the residual vegetation cover formed in previous years. In the presented study, this phenomenon is quantitatively described by the annual saltation flux under the influence of vegetation cover. The effects of precipitation and temperature are introduced by the linear growth model of the plant. Combining with wind speed, a non-dimensional climatic index for aeolian desertification is established. The trend analysis of dust storms frequent confirms that this climatic index is practical.

## Acknowledgement

We are grateful to Kai Yang for downloading meteorological data. This research was supported by the National Key Research and Development Program of China project (No. 2020YFA0608404) and the Natural Science Foundation of China projects (Nos. 41630747 and 41971011).

## Authors' contributions

All authors contributed equally.

## Data availability

The datasets used and/or analyzed during the current study are available from the corresponding author on reasonable request.

## Conflicts of Interest

The authors declare no conflicts of interest.

## REFERENCES

- Giannini A, Biasutti M, Verstraete MM. A climate model-based review of drought in the Sahel: Desertification, the re-greening and climate change. *Global and Planetary Change*. 2008;64(3):119-128.
- Pelletier JD, Murray BA, Pierce JL, Bierman PR, Breshears DD, Crosby BT, et al. Forecasting the response of Earth's surface to future climatic and land use changes: A review of methods and research needs. *Earth's Future*. 2015;3(7):220-251.
- Huang J, Yu H, Guan X, Wang G, Guo R. Accelerated dryland expansion under climate change. *Nature Climate Change*. 2016;6(2):166-171.
- Koutroulis AG. Dryland changes under different levels of global warming. *Science of the Total Environment*. 2019;655:482-511.
- Mabbutt JA. Desertification indicators. *Climatic Change*. 1986;9(1):113-122.
- Huang J, Li Y, Fu C, Chen F, Fu Q, Dai A, et al. Dryland climate change: Recent progress and challenges. *Reviews of Geophysics*. 2017;55(3):719-778.
- Zhang C, Wang X, Li J, Hua T. Identifying the effect of climate change on desertification in northern China *via* trend analysis of potential evapotranspiration and precipitation. *Ecological Indicators*. 2020; 112:106141.
- Zhang C, Wang X, Li J, Zhang Z, Zheng Y. The impact of climate change on aeolian desertification in northern China: Assessment using aridity index. *Catena*. 2021;207:105681.
- Wang X, Chen F, Hasi E, Li J. Desertification in China: An assessment. *Earth-Science Reviews*. 2008;88(3):188-206.
- Wang T. Aeolian desertification and its control in northern China. *International Soil and Water Conservation Research*. 2014;2(4):34-41.
- Wang X, Yang Y, Dong Z, Zhang C. Responses of dune activity and desertification in China to global warming in the twenty-first century. *Global and Planetary Change*. 2009;67(3):167-185.
- Guan Q, Sun X, Yang J, Pan B, Zhao S, Wang L, et al. Dust storms in northern China: Long-term spatiotemporal characteristics and climate controls. *Journal of Climate*. 2017;30(17):6683-6700.
- Huang J, Li Y, Fu C, Chen F, Fu Q, Dai A, et al. Dryland climate change: Recent progress and challenges. *Reviews of Geophysics*. 2017;55(3):719-778.
- Lettau K, Lettau H. Experimental and micrometeorological field studies of dune migration. *Exploring the World's Driest Climate*. Center for Climatic Research, University of Wisconsin, Madison. 1978; 110-147.
- Fryberger S, Dean G. Dune forms and wind regime. In: McKee, E. (Ed.), *A study of global sand seas*. United States government printing office, 1979; 137-169.
- Shen Y, Zhang C, Huang X, Wang X, Cen S. The effect of wind speed averaging time on sand transport estimates. *Catena*. 2019;175: 286-293.
- Yizhaq H, Xu Z, Ashkenazy Y. The effect of wind speed averaging time on the calculation of sand drift potential: New scaling laws. *Earth and Planetary Science Letters*. 2020;544:116373.
- Sherman DJ, Li B, Ellis JT, Swann C. Intermittent Aeolian saltation: A protocol for quantification. *Geographical Review*. 2018;108(2):296-314.
- Lancaster N, Baas A. Influence of vegetation cover on sand transport by wind: field studies at Owens Lake, California. *Earth Surface Processes and Landforms*. 1998;23(1):69-82.
- Paine CET, Marthews TR, Vogt DR, Purves D, Rees M, Hector A, et al. How to fit nonlinear plant growth models and calculate growth rates: an update for ecologists. *Methods in Ecology and Evolution*. 2012;3(2):245-256.
- Gao Q, Yu M. A model of regional vegetation dynamics and its application to the study of Northeast China Transect (NECT) responses to global change. *Global Biogeochemical Cycles*. 1998;12(2):329-344.
- Zhao W, Liu B. The response of sap flow in shrubs to rainfall pulses in the desert region of China. *Agricultural and Forest Meteorology*. 2010;150(9):1297-1306.
- Zhou Z, Wang X. Analysis of the severe group dust storms in eastern part of northwest China. *Journal of Geographical Sciences*. 2002;12(3):357-362.
- Zhou Z, Zhang G. Typical severe dust storms in northern China during 1954-2002. *Chinese Science Bulletin*. 2003;48(21):2266-2370.
- Wang X, Dong Z, Zhang J, Liu L. Modern dust storms in China: an overview. *Journal of Arid Environments*. 2004;58(4):559-574.
- Wang X, Zhou Z, Dong Z. Control of dust emissions by geomorphic conditions, wind environments and land use in northern China: An examination based on dust storm frequency from 1960 to 2003. *Geomorphology*. 2006;81(3):292-308.
- Liu Y, Wang G, Hu Z, Shi P, Lyu Y, Zhang G, et al. Dust storm susceptibility on different land surface types in arid and semiarid regions of northern China. *Atmospheric Research*. 2020;243:105031.